

Wind tunnel experiments of air flow patterns over nabkhas modeled after those from the Hotan River basin, Xinjiang, China (I): non-vegetated

Zhizhong LI (✉)¹, Shengli WU¹, Janis DALE², Lin GE¹, Mudan HE¹, Xiaofeng WANG¹, Jianhui JIN¹, Rong MA¹, Jinwei LIU¹, Wanjuan LI¹

¹ School of Geography Science and Tourism, Xinjiang Normal University, Urumqi 830054, China

² Department of Geology, University of Regina, Regina, SK Canada S4S 0A2

© Higher Education Press and Springer-Verlag 2008

Abstract A nabkha is a vegetated sand mound, which is typical of the aeolian landforms found in the Hotan River basin in Xinjiang, China. This paper compares the results of a series of wind tunnel experiments with an on-site field survey of nabkhas in the Hotan River basin of Xinjiang. Wind tunnel experiments were conducted on semi-spherical and conical sand mounds without vegetation or shadow dunes. Field mounds were 40 times as large as the size of the wind tunnel models. In the wind tunnel experiments, five different velocities from 6 to 14 m/s were selected and used to model the wind flow pattern over individual sand mound using clean air without additional sand. Changes in the flow pattern at different wind speeds resulted in changes to the characteristic structure of the nabkha surface. The results of the experiments for the semi-spherical sand mound at all wind velocities show the formation of a vortex at the bottom of the upwind side of the mound that resulted in scouring and deposition of a crescentic dune upwind of the main mound. The top part of the sand mound is strongly eroded. In the field, these dunes exhibited the same scouring and crescentic dune formation and the eroded upper surface was often topped by a layer of peat within the mound suggesting destroyed vegetation due to river channel migration or by possible anthropogenic forces such as fuel gathering, etc. Experiments for the conical mounds exhibit only a small increase in velocity on the upwind side of the mound and no formation of a vortex at the bottom of the upwind side. Instead, a vortex formed on the leeward side of the mound and overall, no change occurred in the shape of the conical mound. In the field, conical mounds have no crescentic dunes on the upwind side and no erosion at the top exposed below peat beds. Therefore, the field and

laboratory experiments show that semi-spherical and conical sand mounds respond differently to similar wind conditions with different surface configuration and development of crescent-shaped upwind deposits when using air devoid of additional sediment.

Keywords nabkha, sand mounds, wind tunnel experiment, wind flow pattern

1 Introduction

The nabkha, an aeolian landform, is a vegetated sand mound made of small fragments (grit, powdered grit, salt crystal grains, and clay) common in arid, semi-arid and sub-humid environments in deserts along coasts and on valley floors (Zhu and Wu, 1981; Wu, 2003). Wind velocity, availability of fine-grained materials conducive to aeolian transport and the presence of vegetation are the main factors that influence the development of nabkhas. A nabkha often develops a characteristic single lee or shadow dune on the leeside of the vegetation, the shape of which depends on the plant width and slope angle of the sand surface (Hesp, 1981). Shadow dunes form on the leeside from the deposition of wind-blown sand by a strong reverse airflow (Hesp, 1981). Over the last 20 years, the relationship between dune-shape and aeolian processes has been studied through field observations and wind-tunnel experiments for some dune types. This includes research on the characteristic of airflow patterns on the upwind slope of transverse dunes, the relation between airflow and sand transport rates and the impact of secondary flow on leeward dune slope (Tseo, 1993; Stam, 1997; Walker, 1999). Zhang and Chen (1999) simulated surface airflow patterns over the linear dunes in the centre of the Taklimakan Desert in Xinjiang, China.

Translated from *Journal of Desert Research*, 2007, 27(1): 9–14 [译自: 中国沙漠]

E-mail: lzzxj@xjnu.edu.cn

Wang et al. (2004) obtained additional information on the airflow dynamics and resultant shape of simple transverse dunes in the central Taklimakan Desert.

Although the change in shape of nabkhas has been simulated in the earlier wind-tunnel experiments (Zhu et al., 1994), a study of the flow pattern of nabkha using clean air devoid of additional sand has not been reported before. It is important to understand the dynamics of airflow and sand movement in both horizontal and vertical dimensions in order to understand the development of sand dunes. This paper compares the results of a series of wind tunnel experiments with a field survey of nabkhas in the Hotan River basin, Xinjiang Uygur Autonomous Region of Northwestern China. Wind tunnel experiments were conducted on semi-spherical and conical sand mounds without vegetation or shadow dunes. The results provide useful data on the dynamic nature of nabkha shape development.

2 Wind tunnel experiments

2.1 Experimental design

Experiments were conducted in a ‘blowing-type’ soil deflation wind tunnel at the Desert Experiment Station of the Key Laboratory of Desert and Desertification of the Chinese Academy of Sciences, Ningxia Hui Autonomous Region of Northwestern China.

The reliability of wind-tunnel experiments depends on the degree of similarity between experimental results and field conditions. To test this, there are two aspects that are considered in these experiments, i.e. the shape and size of an individual nabkha and airflow patterns, and the wind flow velocity. It is assumed that sand mounds observed in the field were formed under similar conditions to the wind tunnel experiments. Results of measurements of the wind velocity and the shape of the nabkhas in the field were referred to in the laboratory during the simulation (Liu, 1995; Wu, 2003). Thus, the simulated sand mounds will assimilate to the size and shape to those seen in the field and develop under similar aeolian processes over the similar time span. Wind tunnel experiments were conducted with clean airflow and no additional sand source was added to the experimental system. The wind velocity used was similar with the field.

At the field site, *Tamarix* shrubs are commonly associated with the nabkha in the basin of the Hotan River in Xinjiang. In the experiment, models of sand mounds were formed without vegetation to eliminate the influence of plant. Based on the side view, the geometric shapes of nabkhas in the Hotan River Basin are generally divided into semi-spherical and conical shapes, with the lengths of upwind slopes of most of the sand mounds shorter than the leeward slopes (Fig. 1(A) and (B); Table 1).

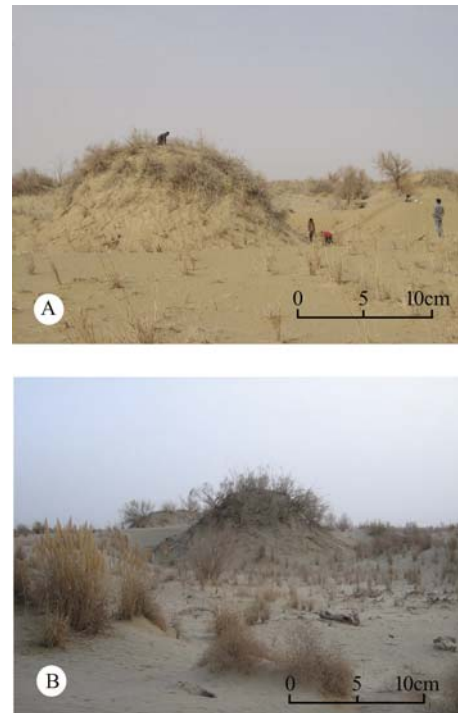


Fig. 1 Nabkhas in the Hotan River basin, Xinjiang, China (A) Semi-spherical nabkha; (B) Conical nabkha

The average height of semi-spherical nabkhas without *Tamarix* shrub is 4.74 m and the average diameter at the base is 12.73 m. In order to simplify the experiment, the difference of slope-length between upwind and leeside is ignored. The experimental semi-spherical nabkha models are constructed of wood which is proportional to the field size at a ratio of 40:1 with a diameter (D_1) of 32 cm, and height (H_1) of 12 cm. The average height of conical nabkhas without *Tamarix* shrub in the field is 5.10 m and the average base diameter is 11.95 m. Likewise, wooden models of conical nabkhas were made at a 40:1 ratio with an average diameter (D_2) of 30 cm and height (H_2) of 13 cm in the experiments (Fig. 2(A) and (B)).

2.2 Experimental methods

The experiments were conducted in a ‘blowing-type’ soil deflation wind tunnel. The wind tunnel has a working section that is 21 m long, 1.2 m wide and 1.2 m high set at an angle less than 1° with upwind-ward. The bottom of the wind tunnel is made of seven moveable alloy aluminum plates which can be easily assembled and disassembled while extending the range of potential experiments. Data are automatically imported into a PC computer from sensors that measure air temperature using a digital thermometer and atmospheric pressure with an aneroid barometer mounted within the working section. The airspeed of the working section is gathered by a wind velocity profile collector which gathers data

Table 1 Measurements of nabkha without *Tamarix* shrub surveyed in the Hotan River Basin of Xinjiang Province

Nabkha Field number	Height/m	Diameter/m	Shape of upwind slope		Shape of leeward slope		Approximate Geometric shape	
			Slope length/m	Slope Gradient/°	Slope Length/m	Slope Gradient/°		
G3B	4.254	8.35	5.44	45	6.87	43	Semi spherical	
G5B	2.475	9	3.7	31	6.52	28		
G8B	3.447	8.4	7.5	33	5.5	31		
G14B	2.698	8.3	5	32	5.5	30		
G16B	9.335	25	13	38	16	42		
G19B	6.208	17.3	10.1	41	10.7	33		
Average	4.74	12.73	7.46	36.67	9.12	34.5		
G9B	4.356	10.6	8.2	37	8.1	28		Conical
G10B	4.595	12.1	8.8	37	7.62	31		
G11B	3.012	7.6	5.6	38	5.04	31		
G12B	5.66	11.4	9	35	6.7	46		
G13B	5.042	11	8.6	40	7.8	36		
G15B	7.932	19	13.45	36	13	38		
Average	5.10	11.95	8.94	37.17	8.04	35		

automatically every 2 seconds over a total collecting time of 60 seconds. The resultant air velocity is the average results collected over the 60 seconds. The maximum wind velocity controlled is 29 m/s by the fan rating.

Sand collected from the field was glued onto the surface of the wooden sand mound models to duplicate the roughness of the field nabkha. Measurements of the airflow patterns over the semi-spherical and conical sand mounds were determined using the following procedure: 1) the models are placed along the main axis of the work section, and the air velocity measuring points are distributed

along the mid-point line of the sand mound model; 2) measurements were taken along the line at the bottom and middle of the upwind slope, the top of the mound and the middle and bottom of the leeward slope of the conical and semi-spherical mounds, and 3) 18 other measuring points were selected along the line upwind and downwind of the semi-spherical mound at 6, 12, 18, 24, 36, 60, 120, 180, and 240 cm distances.

For the conical models, the 18 other measuring points were made at 6.5, 13, 19.5, 26, 39, 65, 130, 195 and 260 cm upwind and downwind distances. Ten measurements were made at each point above the sand surface at 0.3, 0.6, 1.0, 3.0, 6.0, 12.0, 20.0, 35.0 and 50.0 cm to measure the wind velocity profile for both the semi-spherical and conical models (Qu et al., 1992; Li and Chen, 1995; Li and Guan, 1996; Ling et al., 1997; Zhang et al., 1998; Hasi et al., 2000; Hu et al., 2002; Liu and Dong, 2002; Ling et al., 2003; Liu and Dong, 2003). From previous field observations and experimental results, the minimum wind speed required to initiate sand movement is 6 m/s. Experimental air speeds in the working section of the wind tunnel were run at 6, 8, 10, 12, 14 m/s (V_1 – V_5) in order to survey the flow pattern with different wind speeds over the models. Flow patterns of semi-spherical and conical models are drawn using the Surfer (R) 8.0 software package. In this paper, airflow patterns are shown for semi-spherical and conical sand mounds at air velocities of 6, 10 and 14 m/s (Fig. 3).

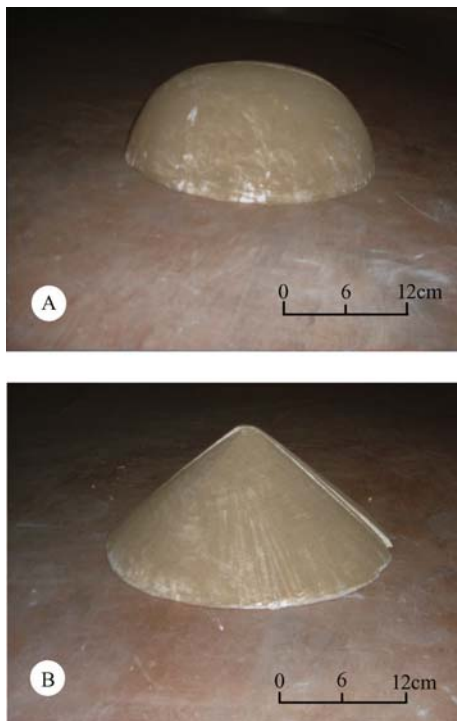


Fig. 2 Nabkha models without vegetation in the wind tunnel (A) Semi-spherical model; (B) Conical model

3 Results

3.1 Airflow patterns over semi-spherical sand mounds

From the experimental results, the airflow pattern over semi-spherical sand mound at different wind speeds can be divided into three areas. The first is a reflected and accelerated vortex area in the front of upwind slope of

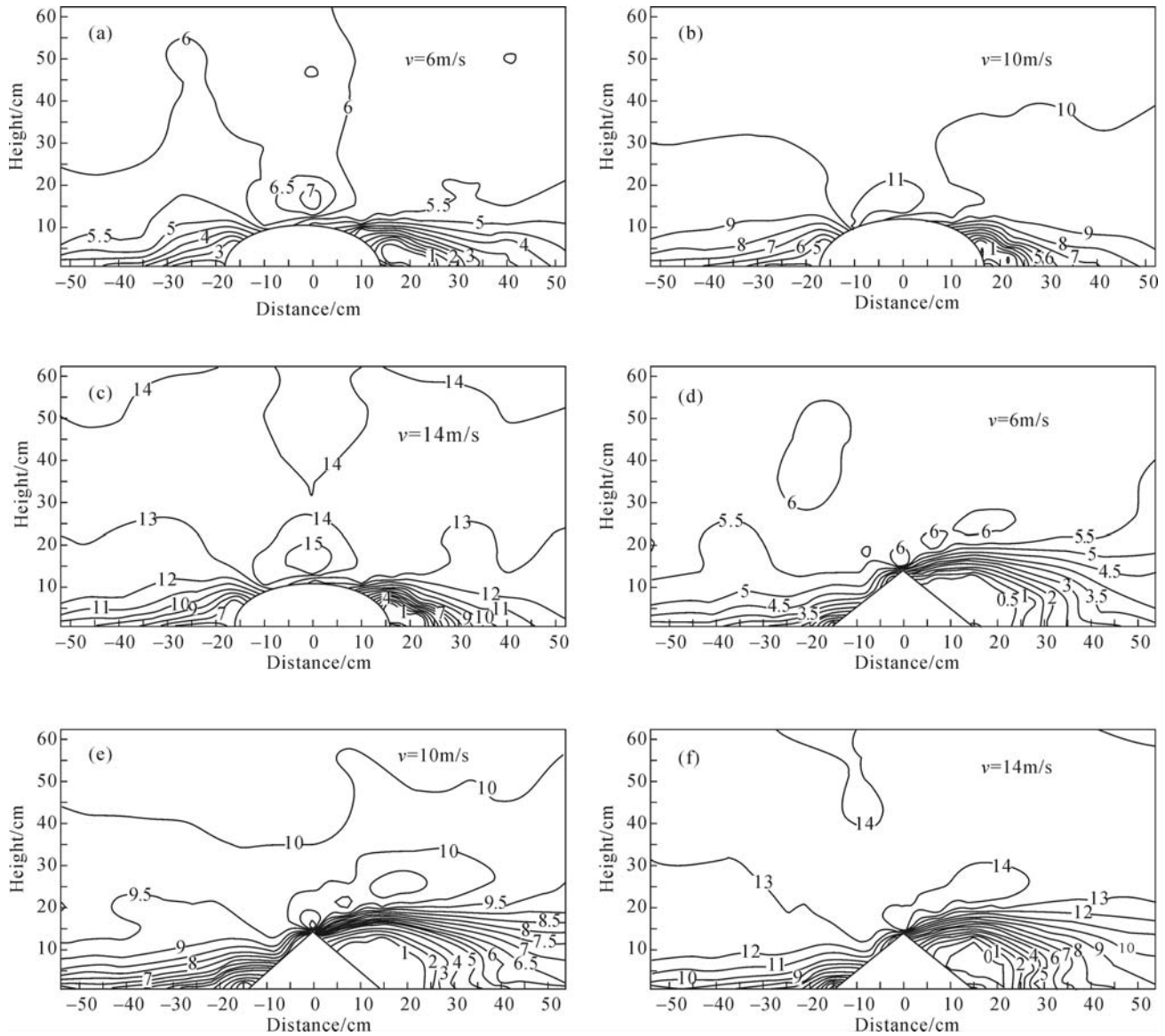


Fig. 3 The flow patterns of different morphological sand mound at three wind speeds. (a)–(c), semi-spherical sand mound; (d)–(f), conical sand mound

the sand mound. The second is a high velocity area at the top of the sand mound and the final is a weak wind vortex area at the leeward slope of the sand mound (Fig. 3(a), (b) and (c)).

A reflected vortex forms at the base of the upwind slope of the semi-spherical sand mound. Its height reaches half the height of the sand mound ($1/2 H_1$) and then thins gradually in an upwind direction. The distance over which the vortex extends ranges in length from 1 to 2 times the height of the mound ($1-2H_1$). The width of the vortex in the front of upwind slope is about one quarter of the height ($1/4 H_1$). The wind-speed of the reflected vortex area is less than half of the average velocity within the working section ($\leq 1/2 v_{1-5}$). The forward airflow encounters resistance from the steep gradient at the bottom of the semi-spherical sand mound so that airflow is reflected

backwards to form the vortex. Within the $1/4 H_1$ distance in front of the mound, sand would not be deposited, but would be eroded by the high velocity of the airflow. This eroded area follows the contours of the mound to form an arc-like shape. Deposition of sand could occur mainly within $1/4 H_1$ to $1 H_1$ distance in front of the semi-spherical sand mound forming a crescent-shaped sand dune.

Semi-spherical sand mounds form in areas with a sufficient sand source in the Hotan River basin. The formation of crescent-shaped dunes and area of erosion at the foot of the upwind slope of semi-spherical sand mounds was observed in the field and was due to the formation of a strong reflected vortex. In the experiments, despite an increase in air-velocity, the size of the reflected vortex in the front of the semi-spherical model did not change. It appears that the size of the reflected vortex is not related

to air speed but related to the size of the semi-spherical nabkha. This is confirmed through observations in the Hotan River basin where for each individual nabkha, the size of the crescent-shaped dune, the depth of the eroded arc-shaped area and the size of the semi-spherical nabkha are proportional to one another. The relationship between landform shape and the aeolian processes of simple transverse dunes has been studied in the Taklimakan Desert in China. It was determined that the shape and size of the simple transverse dune maintains a closer relationship (Wang et al., 2004). For the semi-spherical model, airflow accelerates at a distance of $1/2 H_1$ on the upwind slope of the model. In the middle of the reflected-vortex, the wind-speed is less than 1 m/s and increases towards the top of the semi-spherical model. The greatest increase in wind-speed occurs within the area above $\geq 1/2 H_1$ on the top surface and along the sides of the semi-spherical model. These areas of the sand mound are susceptible to wind-erosion when the vegetation is removed or dies. An increase in velocity on upwind slopes towards the top is a common phenomenon and found with linear and simple transverse dunes in the centre of the Taklimakan desert (Zhang and Chen, 1999; Wang et al., 2004).

The zone of high wind velocity at the top of the semi-spherical model has a diameter of $2/3 D_1$ of the sand mound and a vertical thickness up to $1 H_1$. This zone has a velocity 1–2 m/s greater than the average selected experimental velocity. The airflow accelerates steeply along the upwind slope, reaching its maximum at the top of the sand mound. Based on field observations in the Hotan River basin, the grain size of sand at the top of the nabkha is coarser than other parts of the mound. After the loss or decay of vegetation, an irregular wind-erosion pit forms at the top of the sand mound that leads to the degradation of the semi-spherical nabkha (Fig. 4).

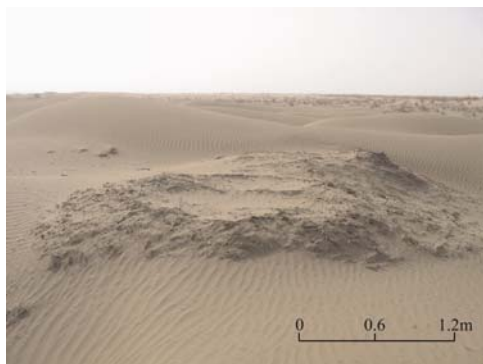


Fig. 4 Landscape of wind eroded nabkhas. Note the wind-erosion pits formed on the top of the sand mounds

In the experiment, the formation of a high velocity area at the top of the semi-spherical model could account for the coarsening of grain size and formation of a wind-erosion pit at the top of the sand mound. Through field

observations, the coarse grain size and irregular wind-erosion pit at the top of the nabkha verifies the existence of a high velocity flow over the top area. Different airflow patterns have been observed at the top of other types of dunes. Wiggs et al. (1996) found that as airflow reaches the top of simple transverse dunes, obstacles at the top reduce airflow resulting in the accumulation of sand.

There is a weak wind vortex area at the leeward slope of the semi-spherical model. The central area of the vortex clings to the foot of the leeward slope. The vortex reaches a thickness of $1/2$ – $2/3 H_1$ of the model and covers a distance of 3 – $4 H_1$ downwind. The airflow around and over the semi-spherical model converges and decelerates at the leeside. The lowest velocity occurs at the foot of the leeward slope and accelerates slowly until it resumes the experimental wind speed. These results are well with our present understanding of leeward wind movement over dunes (Zhang and Chen, 1999) although the size of the leeward vortex can vary. Wang et al., (2004) found the length of the vortex on the leeside of simple transverse dunes to be 12 times the height of the dune.

3.2 Airflow patterns over conical sand mounds

From the wind tunnel experiments, the airflow pattern of conical sand mound at different speeds can be divided into three zones: an area of accelerating wind on the upwind slope, a weak vortex at the top and a strong vortex on the leeward slope (Figs. 3.(d), (e) and (f)).

The area of accelerating air on the upwind slope of conical sand mounds is different from the semi-spherical model. Airflow accelerates equably along the upwind slope below the $1/2 H_2$, with little to no vortex formation. The speed of airflow stabilizes at about $2/3$ of the experimental wind-speed over $1/2 H_2$ on the upwind slope. As the airflow approaches the top of the conical sand mound model, airflow velocity increases to the experimental speed. In the Hotan River basin in the front of vegetated (*Tamarix*) conical nabkha, the reflected crescent-shaped dune and erosion sand arc are not present even in the areas with sufficient sand.

A weak vortex forms at the top of the conical sand mound. At lower experimental wind speeds, several smaller vortices form, which reaches the same speed as the given velocity. The sharp point at the top of the conical sand mound limits the available surface area and thus reduces the influence of these vortices on the mound itself. The length of the weak vortex area extends to 1 – $2 H_2$ of the model downwind, with a thickness reaching $1 H_1$. The average wind-speed of the weak vortex area at the top of the conical sand mound model depends on the experimental wind-speed and is not influenced by acceleration on the upwind side. The weak vortex area changes with airflow velocity becoming larger with increasing speed. Overall, the air-speed of the vortex is lower for the conical mound than that of the

semi-spherical sand mound under the same wind speeds. Based on observations in the Hotan River basin after plants have been destroyed, wind-erosion and degradation is initiated. During this initial stage, the conical nabkha maintains the conical shape on the whole although the height of the nabkha is rapidly reduced by wind erosion at the top.

A strong vortex area develops at the leeside of the conical sand mound at the point at which the airflow passing over and around where the conical sand mound joins. The air speed declines rapidly from the experimental wind speed at the top to less than 1 m/s in the middle of the vortex. The thickness of the vortex is over 1 H_2 and the vortex area extends over 2–3 H_2 in a downwind direction. The core vortex area with a velocity less than 1 m/s has a thickness of $2/3 H_2$ and extends for a length of $3/4 H_2$ in the downwind direction on the leeside. All airflow velocity values begin to increase at roughly $1/2 H_2$ from the foot of the leeward slope in the downwind direction and approach the experimental wind speed. The conical nabkha appears to quickly reach a balance between airflow and shape regardless of increasing wind velocity.

4 Conclusions

Using a series of wind tunnel experiments and a field survey of nabkhas in the Hotan River basin, two-dimensional airflows pattern of semi-spherical and conical sand mounds were examined. The sand mounds in the field and wind tunnel experiments were devoid of vegetation and shadow dunes. The main results can be summarized as follows:

(1) The airflow pattern over a semi-spherical sand mound is divided into three areas: 1) reflected and accelerated vortex area on the upwind slope; 2) high velocity area at the top, and 3) weak wind vortex area at the leeward slope. The reflected and accelerated vortex on the upwind slope accounts for the formation of the crescent sand dune and area of erosion that forms an arc-shape at the foot in front of the semi-spherical sand mound observed in the field.

(2) The airflow circulation observed for the conical sand mound is separated into three zones: accelerating area on the upwind slope, weak vortex area at the top and strong vortex area on the leeside. Unlike the semi-spherical model, no reflected and accelerated vortex formed on the upwind slope making it unlikely that a crescent-shaped sand dune or eroded arc would be formed in front of the foot of the upwind slope of the conical nabkha. The same observation was made in the field where no crescent-shaped dune or erosion area was observed.

(3) The geometric shape of the sand mound affects the airflow motion and development of vortices. Comparing

the airflow pattern between semi-spherical and conical sand mounds a number of differences were apparent. The vortex that forms in the front of upwind slope is more powerful for the semi-spherical sand mound and rarely observed for the conical mound. An erosion area of high velocity forms at the top of the semi-spherical mound. A weak vortex of less erosion develops at the top of the conical model. The semi-spherical mound has a weak vortex at the leeward slope in comparison to the more powerful vortex that forms with the conical sand mound.

(4) The results of the wind tunnel experiments confirm observations made in the field in the Hotan River basin. The loss of vegetation affects the rate of erosion particularly at the top the semi-spherical sand mound where a pit is gradually formed. However, erosion is not obvious at the top of conical sand mounds which appear to reach equilibrium relatively quickly due to airflow velocity, erosion which gives the resultant conical shape of the mound.

Acknowledgements This work was supported by the National Natural Science Foundation of China (Nos. 40461002,40761004), the Key Science and Technology Project of the Ministry of Education (No. Region 205184) and the Key Project of Universities Plan Science Foundation of Xinjiang Uygur Autonomous Region (No. XJEDU2004135).

References

- Hasi, Wang G Y, Dong G R (2000). Geomorphological significance of air low over reticulate dunes of the southeastern Tengger desert. *Journal of Desert Research*, 20(1): 30–34 (in Chinese)
- Hesp P A (1981). The formation of shadow dune. *Journal of Sedimentary Petrology*, 51: 101–112
- Hu M C, Zhao A G, Li N (2002). Sand-trapping efficiency of railway protective system in Shapotou tested by wind tunnel. *Journal of Desert Research*, 22(6): 598–602 (in Chinese)
- Li Z Z, Chen G T (1995). Experimental study on the structure of wind-tunnel flow pattern for Pyramid dune: giving consideration to a model for Pyramid dune formation. *Journal of Desert Research*, 15(3): 227–233 (in Chinese)
- Li Z Z, Guan Y Z (1996). Experimental study on imitative flow pattern of longitudinal and transverse dunes. *Journal of Desert Research*, 16(4): 360–363 (in Chinese)
- Ling Y Q, Liu S Z, Wu Z et al (1997). Analysis on dynamics conditions of Pyramid dunes formation. *Journal of Desert Research*, 17(2): 112–118 (in Chinese)
- Ling Y Q, Qu J J, Jin J (2003). Influence of sparse natural vegetation on sand-transporting quantity. *Journal of Desert Research*, 23(1): 12–18 (in Chinese)
- Liu X P, Dong Z B (2002). Wind tunnel tests of the roughness and drag partition on vegetated surfaces. *Journal of Desert Research*, 22(1): 82–88 (in Chinese)
- Liu X P, Dong Z B (2003). Aerodynamic roughness of gravel beds. *Journal of Desert Research*, 23(1): 38–46 (in Chinese)
- Liu X W (1995). *Experimental physics and engineer of wind-sand experiment*. Beijing: Science Press, 66–68 (in Chinese)
- Qu J J, Lin Y Q, Zhang W M et al (1992). Preliminary observation and study on the formation mechanism of Pyramid dune. *Journal of Desert Research*, 12(4): 19–27 (in Chinese)
- Stam J M T (1997). On the modeling of two-dimensional Aeolian dunes. *Sedimentology*, 44: 127–141

- Tseo G (1993). Two types of longitudinal dune fields and possible mechanisms for their development. *Earth Surface Processes and Landforms*, 18: 627–643
- Walker I J (1999). Secondary airflow and sediment transport in the lee of a reversing dune. *Earth Surface Processes and Landforms*, 24: 437–448
- Wang X M, Dong Z B, Zhao A G (2004). Air flow and particle-size distributions and their significance on the dynamic process of a simple transverse dune. *Journal of arid land resources & environment*, 18(4): 29–34 (in Chinese)
- Wiggs G F S, Livingstone I, Wancen A (1996). The role of streamline curvature in sand dune dynamics: evidence from field and wind tunnel measurements. *Geomorphology*, (17): 29–46
- Wu Z (2003). *Geomorphology of wind-drift sands and their controlled engineering*. Beijing: Science Press, 400–404 (in Chinese)
- Zhang W M, Li X Z, Qu J J, et al (1998). The flow field and its dynamics process of pyramidal dune. *Journal of desert research*, 18(3): 215–220 (in Chinese)
- Zhang J W, Chen G T (1999). The surface dynamics process of linear dune in central area of Taklimakan desert. *Journal of desert research*, 19(2): 128–134 (in Chinese)
- Zhu Z D, Wu Z (1981). *Study on sand landform in Taklimakan desert*. Beijing: Science Press, 41–48 (in Chinese)
- Zhu Z D, Chen G T, Wang T et al (1994). *Sandy desertification in China*. Beijing: Science Press, 24–25 (in Chinese)